Supplementary material: Carrier Dynamics near a Crack in GaN microwires with AlGaN multiple quantum wells

Sylvain Finot,[1, a)] Vincent Grenier,[2] Vitaly Zubialevich,[3] Catherine Bougerol,[1] Pietro Pampili,[3] Joël Eymery,[4] Peter J. Parbrook,[3] Christophe Durand,[2] and Gwénolé Jacopin[1, b)]

[1)] *Univ. Grenoble Alpes, CNRS, Grenoble INP*, Institut Néel, 38000 Grenoble, France*

[2)] *Univ. Grenoble Alpes, CEA, IRIG, PHELIQS, NPSC, 38000 Grenoble, France*

[3)] *Tyndall National Institute, University College Cork, Cork T12 R5CP, Ireland*

[4)] *Univ. Grenoble Alpes, CEA, IRIG, MEM, NRS, 38000 Grenoble, France*

[a)] sylvain.finot@neel.cnrs.fr

[b)] gwenole.jacopin@neel.cnrs.fr

I. EXPERIMENTAL SETUP

Figure S1 describes the experimental setup consisting of an FEI Inspect F50 field emission electron scanning microscope (FESEM) equipped with an internally developed CL system. A mirror is used to send the light either to the spatially resolved time-correlated CL (SRTC-CL) part (in red) or to the hyperspectral CL part (in green). The SRTC-CL part is composed of two PMA-hybrid 06 from Picoquant connected to the two channels of a Picoharp 300 time correlated single photon counting module (TCSPS). For the hyperspectral part of the setup, the spectra are obtained using a Horiba iHR550 spectrometer and acquired with the Andor Newton DU940 BU2 charge-coupled device (CCD) camera. A Labview program was developed internally for the control and synchronization of the e-beam spot position, the spectrometer and the CCD camera in order to acquire hyperspectral mappings.

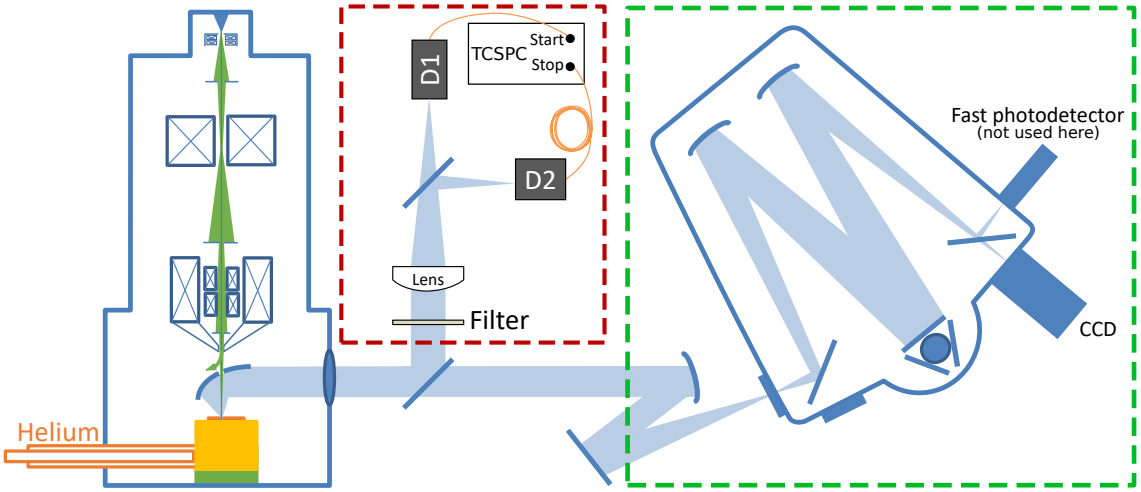

FIG. S1. Schema of the experimental setup. The red box corresponds to the SRTC-CL part and the green one to the hyperspectral CL part.

II. SRTC-CL PRINCIPLE

The spatially resolved time-correlated cathodoluminescence (SRTC-CL) is based on the property that probe electrons create multiple electron-hole pairs due to their high energy relative to the bandgap. If the probe electrons are sufficiently separated in time, typically one electron per lifetime, it is possible to obtain the decay dynamics of the bunches and thus

the effective lifetime τ_{eff} defined as :

$$1/\tau_{eff} = 1/\tau_r + 1/\tau_{nr}$$

Where τ_r (resp. τ_{nr}) is the radiative (resp. non-radiative) lifetime.

The autocorrelation measurement works as follow :

1. When **one** probe electron reaches the sample, it creates a bunch of electron-hole pairs.
2. The pairs recombine either radiatively or non-radiatively with a given effective lifetime.
3. When a photon reaches Detector 1 it starts/resets a clock.
4. When a photon reaches Detector 2, the clock time is stored in a histogram.

To record also the negative delays (i.e. when the first photon arrives on detector 2), it is necessary to add a delay between the two detectors. This is done by adding a 6m cable between D2 and the TCSPC module. The difference in cable length results in an about 26 ns delay between the two detectors.

The obtained histogram can be fitted with the following expression :

$$\begin{aligned} I(t) &= B\left(1 + g_0 \exp\left(-\frac{|t-t_0|}{\tau_{eff}}\right)\right) \\ &\equiv B \cdot g^2(t) \end{aligned}$$

Where B is the baseline which corresponds to the uncorrelated counts between two different incoming electrons, g_0 the value of the autocorrelation function at the added delay t_0 and τ_{eff} the effective lifetime. To obtain the effective lifetime we first divided the histogram by the baseline (its mean at large delays). We then fitted $g^2(t) - 1$ with an exponential decay. More detail about the principle can be found in ref. 1. Figure S2 shows $g^2 - 1$ and the corresponding fits at a distance of 100nm and 1500nm from the crack. The measurements were done at 5K with a 5pA ebeam current and a 2kV acceleration voltage. The linescan was done point by point with a dwell time of about 100s and the sample was realigned between each point thanks to SEM images.

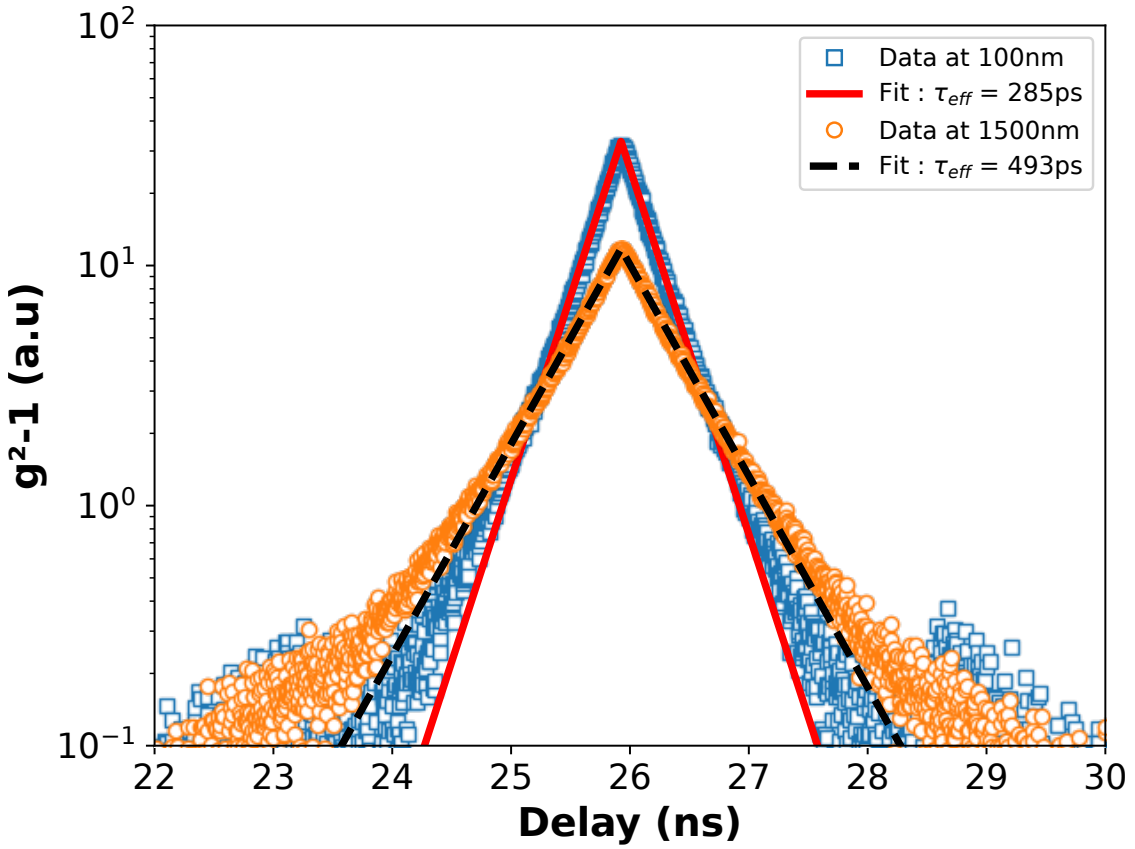

FIG. S2. Measurement of $g^2 - 1$ at two different distances from the crack (data point) and their corresponding fit (lines). The blue squares and the solid red line (resp. orange circles and dashed black line) corresponds to a distance of 100nm (resp. 1500nm) from the crack.

III. TIMING RESOLUTION ESTIMATION

The full width at half maximum (FWHM) of the transit time of a PMA Hybrid 06 is given by Picoquant as typically less than 50 ps. If we take the worst-case scenario, assuming that each detector has a FWHM of 50 ps, the resulting timing resolution for the correlation should be $\sqrt{2} \times 50 \approx 71$ ps. Here, we have estimated the resolution by fitting measurements done at $300K$ (*i.e* with short lifetime) using an exponential decay convolved with a gaussian. Data have been fitted with several fixed FWHM (dashed lines) and without fixing the FWHM (red solid line). We can see that a 70 ps FWHM is too broad at a lower delay and declines too rapidly. On the other hand, it is not easy to distinguish between 20 and 40 ps. Therefore, the resolution should be typically better than 40 ps.

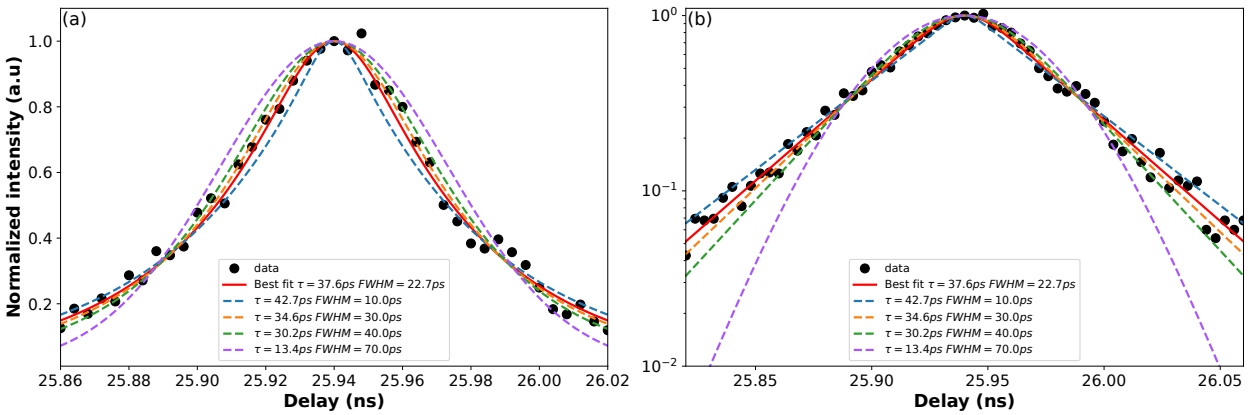

FIG. S3. Normalized histogram obtained with the HBT setup at 300K in linear scale (a) and in logscale (b). Data (black circles) are fitted with an exponential decay convolved with a gaussian. Data have been fitted with several fixed FWHM (dashed lines) and without fixing the FWHM (red solid line).

IV. ADDITIONAL CL MEASUREMENTS

Figure S4 shows the mean spectrum of a 0.25 µm^2 area acquired at $T = 5K$ with a 30kV acceleration voltage. In addition to the multiple quantum wells (MQWs) emission centred

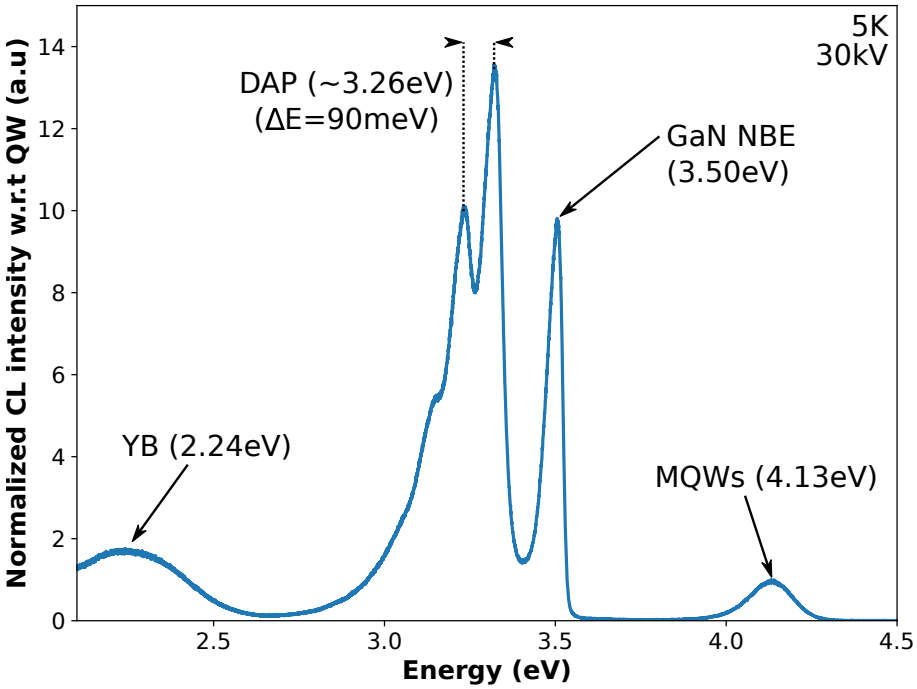

FIG. S4. Spectrum acquired in a 0.25 µm^2 area with a 30kV acceleration voltage at $T = 5K$

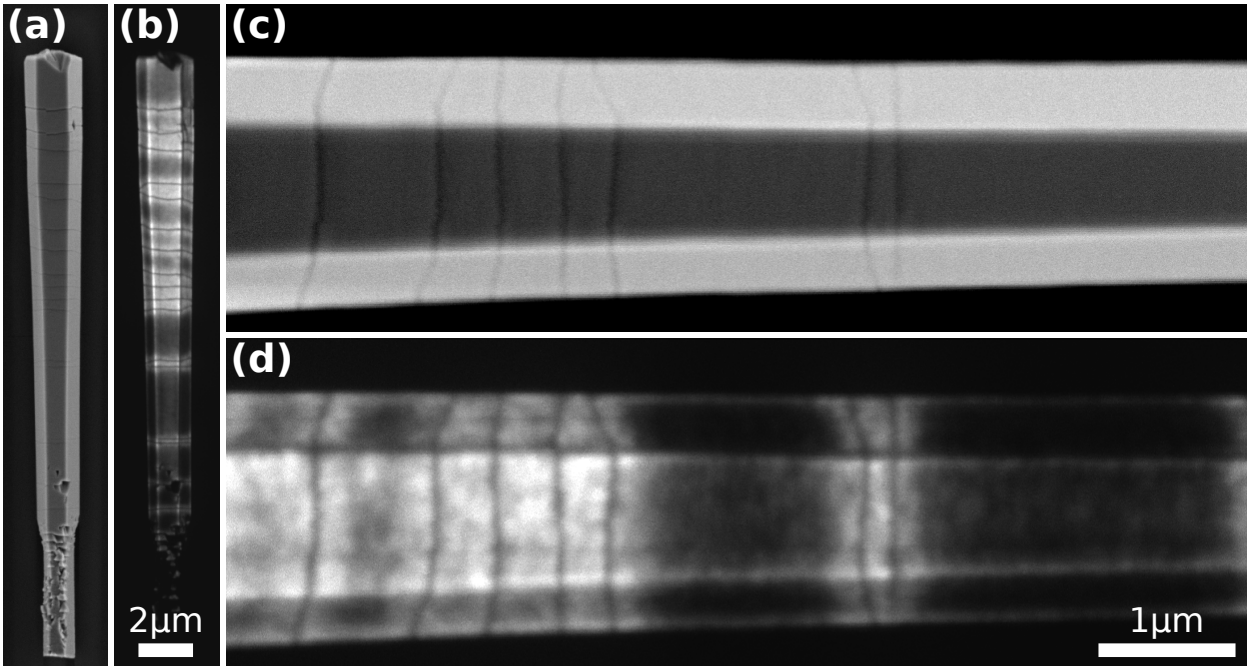

FIG. S5. SEM images of a wire with multiple cracks (a,c) and their corresponding CL images at the MQWs emission (b,d). Both CL and SEM images have been acquired with a 5kV acceleration voltage, at $T = 5K$.

at 4.13 eV with a FWHM of 150 meV, three typical signatures of the GaN core can be identified : the broad yellow band at 2.24 eV, the DAP band around 3.26 eV with 90 meV LO phonon replicas and the near band edge emission (NBE) at 3.5eV.[2]

Additionally to the mapping of the CL spectra presented in Figure 1 of the paper, Figure S5 (a) and (c) shows SEM images and their corresponding monochromatic CL images centered at the MQWs energy. Thanks to this spatial resolution, it is possible to identify the crack in the CL images.

V. PROBING DEPTH

To estimate the probing depth of the CL and SRTC-CL measurements, we used Monte Carlo simulations with the software CASINO.[3] First, we estimated the densities of the $Al_xGa_{1-x}N$ alloys composing the QWs and the barriers assuming that the structure is pseudomorph on m-plane GaN substrate. For the barriers, $x = 0.6$, so the density is estimated to be 4.2 g.cm^{-3}. Respectively, for the QWs with $x = 0.4$, the density should be 4.8 g.cm^{-3}.

Figure S6 shows the projection of the interaction volume obtained at 2 kV onto the a-plane. The QWs and the barriers have a thickness of 4 and 10 nm respectively. Thus, by choosing an accelerating voltage of 2 kV, the radial scattering is low and allows to achieve a spatial resolution better than 50 nm. Moreover, the GaN core is not probed which removes an additional noise source in SRTC-CL. However, only the first three QWs are probed by electrons, so it is important to understand the difference between the different quantum wells in more detail.

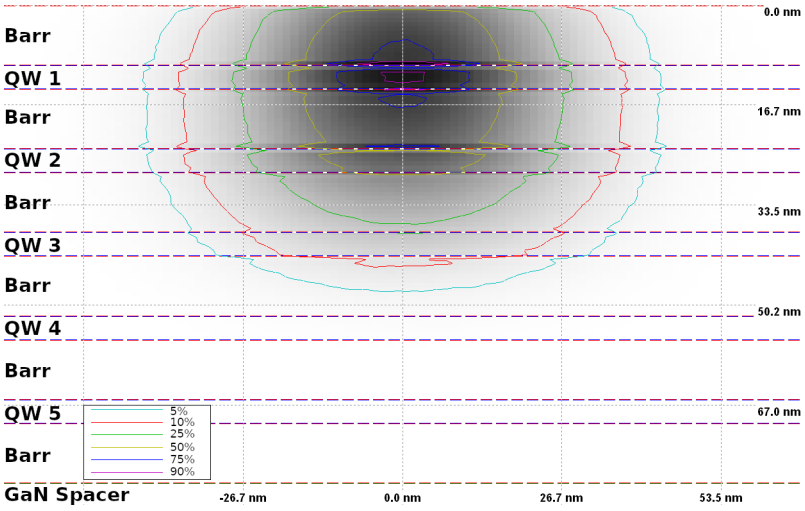

FIG. S6. Projection of the interaction volume at 2 kV onto the a-plane with CASINO

Figure S7 shows the simulated energy in the five QWs for two different distances from the crack. At about 860 nm from the crack, the energy is constant between the different QWs, whereas at about 130 nm, the shift is highly dependent on the distance to the spacer. The main hypothesis is that close to the surface, the structure has two free surfaces (air on the top and crack on the side), whereas close to the spacer, relaxation is only possible thanks to the crack.

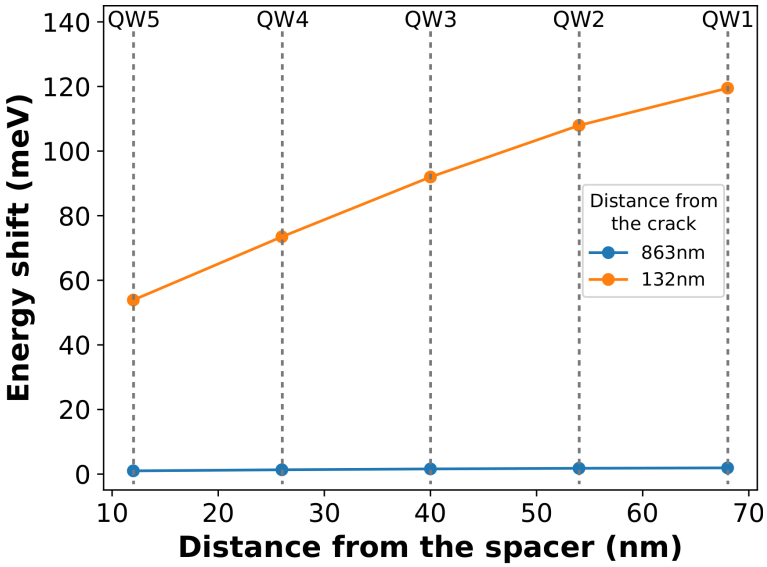

FIG. S7. Cross section of the energy shift along the m-axis for two different distance to the crack

VI. EFFECT OF AL-CONTENT ON THE NEXTNANO3 SIMULATIONS

The effect of Al content has been studied by varying the content from 50 to 40% in the QWs and 75 to 60% in the barriers. Figure S8(a) shows the simulated bandgap energy for an Al content of 50% in the QW and 75% in the barriers as estimated by XRD. Similarly, Figure S8(b) shows the energy shift. It can be seen that the general trend with the simulations performed with 40% and 60% is preserved but the decrease in Al content brings the simulation results closer to the CL observations.

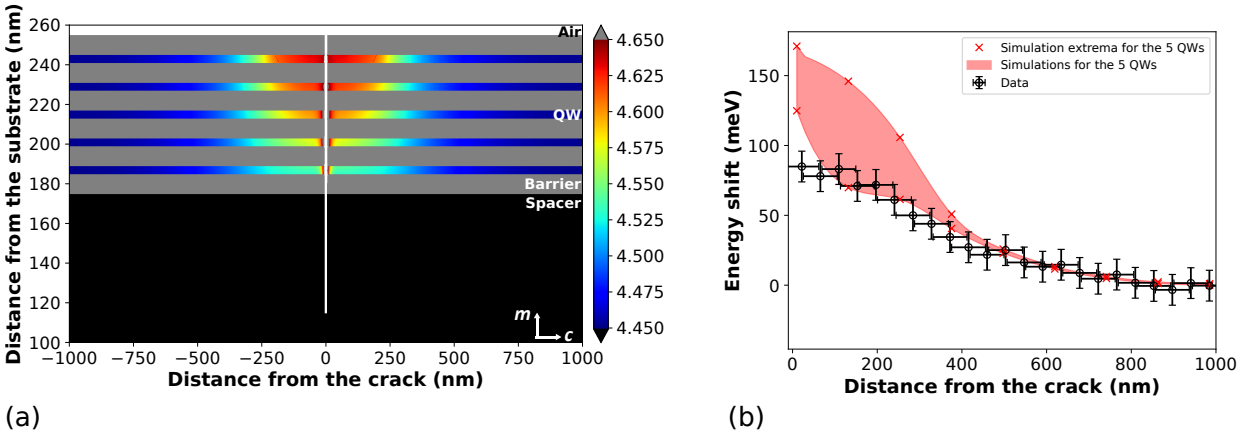

FIG. S8. (a) Mapping of the local bandgap energy in the five QWs near a crack with nextnano3 calculations. The air appears in white, the AlGaN barrier in grey, and the GaN spacer in black.(b) Comparison between simulated and experimental energy shift as a function of the distance to the crack. The simulations correspond to the lowest energy transitions in the obtained by solving Schrödinger equation for both holes and electrons.

VII. QUALITATIVE EDX MEASUREMENTS

Qualitative EDX measurements have been performed in a FEI THEMIS transmission electron microscope operated at 200kV and equipped with super X detectors. Figure S9(a) shows a HAADF-TEM image of a crack with the corresponding EDX intensity map. Figure S9(b) and (c). In the intensity profile of the Ga-KA and Al-K lines shown in Figure S9(d), we can see that Al and Ga intensities are strongly correlated thus we believe that no significant change in Al content is present near a crack. Unfortunately, the measurement could only be done on a thick section of the FIB slice. This may explain why the HAADF-TEM image is not very resolved. It also limited the choice to a poorly defined crack, with the result that the counts associated to Al and Ga are not zero inside the crack.

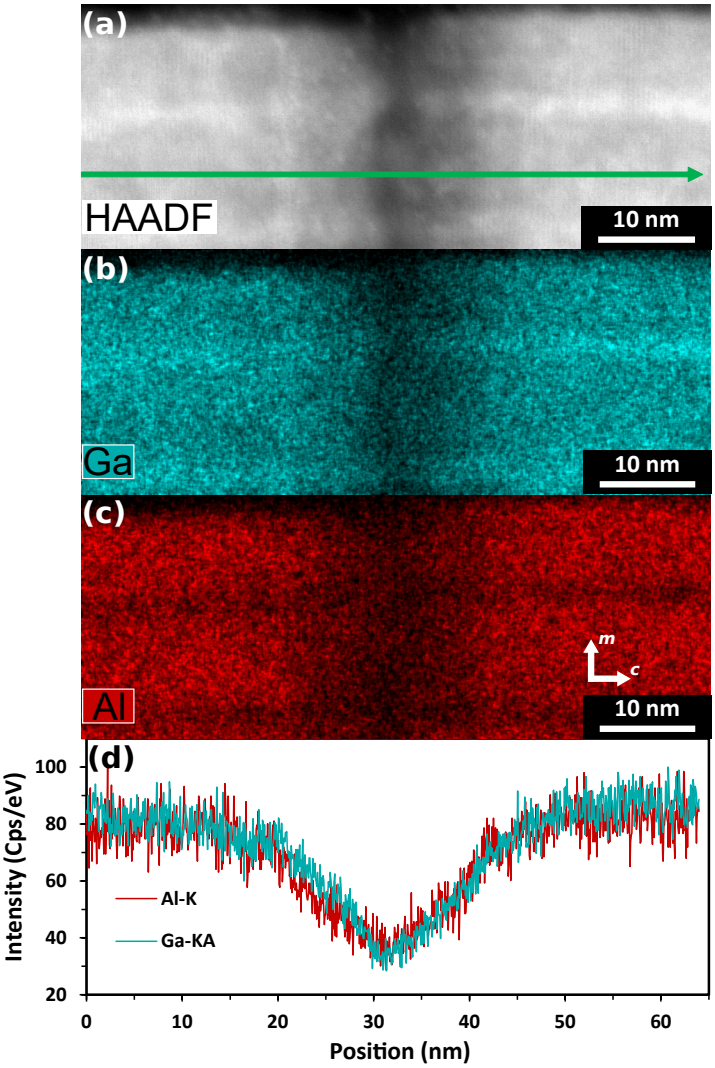

FIG. S9. (a) HAADF-TEM longitudinal cross-section near a crack and the corresponding EDX intensity map of Ga and Al (b) and (c). (d) Intensity profile of Al-K and Ga-KA lines along the c-axis

.

REFERENCES

[S1]S. Meuret, T. Coenen, H. Zeijlemaker, M. Latzel, S. Christiansen, S. Conesa-Boj, and A. Polman, "Photon bunching reveals single-electron cathodoluminescence excitation efficiency in InGaN quantum wells," Physical Review B **96**, 035308 (2017).

[S2]M. A. Reshchikov and H. Morkǫ, "Luminescence properties of defects in GaN," Journal of Applied Physics **97** (2005), 10.1063/1.1868059.

[S3]D. Drouin, A. R. Couture, D. Joly, X. Tastet, V. Aimez, and R. Gauvin, "CASINO V2.42—A Fast and Easy-to-use Modeling Tool for Scanning Electron Microscopy and Microanalysis Users," Scanning **29**, 92–101 (2007).